

# Spatially Modulated Refractive Indices and Optical Filter Characteristics in the Light-Induced Metastable State of $\text{Na}_2[\text{Fe}(\text{CN})_5\text{NO}]\cdot 2\text{H}_2\text{O}^\dagger$

Yoshiyuki Morioka,\* Hideki Saitoh, and Hiroshi Machida

Department of Chemistry, Saitama University, 255 Shimo-Okubo, Saitama 338-8570, Japan

Received: July 17, 2001; In Final Form: November 2, 2001

The metastable state of  $\text{Na}_2[\text{Fe}(\text{CN})_5\text{NO}]\cdot 2\text{H}_2\text{O}$  crystals produced by irradiation with green or blue laser light was investigated using X-ray diffraction and spectroscopic methods. A thin crystalline plate in the metastable state placed between a pair of polarizers behaves like an optical filter. It works as the band-pass or band-reject filter, depending on the cross or parallel alignment of polarizers. A remarkable point of this effect is that the band center corresponds with the wavelength of the laser applied for producing the metastable state. This phenomenon is explained based on spatially modulated refractive indices produced by the photorefractive effect of laser irradiation. Numerical calculations using Berreman's  $4\times 4$  matrix method show that the spatially modulated population of the metastable anion exists even in the photostationary state. Similarity with the Sölc birefringent filter is also discussed.

## I. Introduction

A metastable state of a sodium nitroprusside crystal ( $\text{Na}_2[\text{Fe}(\text{CN})_5\text{NO}]\cdot 2\text{H}_2\text{O}$ , abbreviated to SNP hereafter) is produced when the crystal is exposed in laser light of the blue–green region below 100 K. The new state was first found by Hauser et al. using Mössbauer spectroscopy<sup>1</sup> and has been studied by various techniques such as infrared spectroscopy,<sup>2,3</sup> Raman spectroscopy,<sup>4–6</sup> DSC measurements,<sup>7</sup> X-ray diffractions,<sup>8</sup> and DFT calculations.<sup>9</sup> Results obtained by these investigations are summarized as follows: (1) two new species of the  $[\text{Fe}(\text{CN})_5\text{NO}]^{2-}$  anion are populated upon irradiation with light in the 350–580 nm spectral region at 77 K and vanish thoroughly above 200 K; (2) the two anion species, denoted by  $\text{MS}_1$  and  $\text{MS}_2$ , have extremely long lifetimes and do not show any indication of spontaneous decay below 100 K; (3)  $\text{MS}_1$  and  $\text{MS}_2$  show exothermic decays to the ground state (denoted by GS) above ca. 130 K ( $\text{MS}_2$ ) and ca. 180 K ( $\text{MS}_1$ ); (4)  $\text{MS}_1$  and  $\text{MS}_2$  have higher energies than GS by 1 eV; (5) the photostationary equilibrium is reached by continued irradiation and it controls number densities of  $\text{MS}_1$  and  $\text{MS}_2$ ; (6) the NO group is inverted in  $\text{MS}_1$  and side-bound in  $\text{MS}_2$ ; and (7) similar metastable states are produced in ruthenium- and osmium-nitrosyl complexes.

In 1992, one of the authors (Y.M.) reported an anomalous optical property of an SNP single crystal in its metastable state.<sup>10</sup> First, the metastable state is formed in a *c*-cut SNP single crystal by irradiation with a linearly polarized laser of wavelength  $\lambda_L$  as shown in Figure 1a. Polarization of the laser should be intermediate between the crystallographic *a* and *b* axes, i.e.,  $\chi \neq 0$  and  $\chi \neq \pi/2$ . Next, white light is passed through a system of the metastable SNP crystal and two polarizers as shown in Figure 1b. When the polarizers are crossed and their directions are parallel to the *a* and *b* axes, the spectrum of the transmitted light  $S(\lambda)$  is quasi-monochromatic (solid line in Figure 1c) of wavelength  $\lambda_0$ , whereas  $S(\lambda)$  shows a sharp dip (dashed line) at  $\lambda_0$  when one of the polarizers is rotated by  $90^\circ$ . The wavelength  $\lambda_0$  depends on  $\lambda_L$  and  $\lambda_0 \approx \lambda_L$ . It should be noted that the

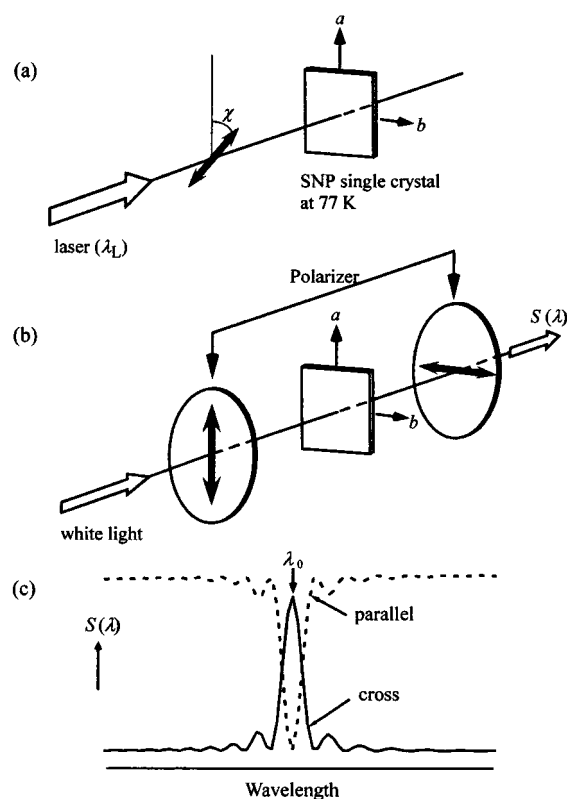


**Figure 1.** Optical filter characteristics of the metastable state of SNP. The metastable state is produced by irradiation with a laser line polarized at an angle  $\chi = 40\text{--}50^\circ$  to the *a*-axis (a); a spectrum  $S(\lambda)$  of light transmitted by the metastable SNP crystal sandwiched between two polarizers is measured (b);  $S(\lambda)$  has a peak or a dip depending on the orientation of the polarizers (c).

SNP crystal before irradiation belongs to the space group  $D_{2h}^{12}\text{-Pnmm}$  of the orthorhombic system and, therefore, light of the whole spectral region is not transmitted through the system of Figure 1b in the crossed polarizers.

In ref 10, to explain the band-pass and band-reject characteristics of the metastable SNP crystal, the author proposed a

<sup>†</sup> Part of the special issue "Mitsuo Tasumi Festschrift".

\* Corresponding author. E-mail: morioka@chem.saitama-u.ac.jp.

mechanism of *accidental isotropy in optically active crystals*, which had been demonstrated for the first time by Hobden in AgGaS<sub>2</sub> as belonging to the optically active  $D_{2d}$  point group.<sup>11</sup> Because SNP belongs to the centrosymmetric  $D_{2h}$  point group in the ground state, a light-induced symmetry change was presumed in ref 10. The assumed symmetry change, however, has remained to be examined experimentally. Another problem raised in ref 10 is to explain the observed relation  $\lambda_0 \approx \lambda_L$ . The theory based on the accidental isotropy in optically active crystals accounts for the optical property shown in Figure 1c qualitatively but does not explain the observed correlation between  $\lambda_0$  and  $\lambda_L$ .

It is a purpose of the present paper to elucidate the optical properties of the metastable state of SNP definitely. For this purpose, we did X-ray diffraction measurements for the metastable state to examine whether a symmetry change to the optically active point group, say  $D_2$ , might happen or not. Then, since results of the X-ray diffraction were negative to the assumed symmetry change, we carried out detailed optical measurements and obtained results that cannot be explained by spatially homogeneous optical properties. Based on these observations, we propose a model involving photorefractive formation of a spatially heterogeneous structure due to laser irradiation and show that the model reproduces not only the band-pass and band-reject characteristics but also a strict equality between  $\lambda_0$  and  $\lambda_L$ .

## II. Experimental Section

Single crystals of Na<sub>2</sub>[Fe(CN)<sub>5</sub>NO]·2H<sub>2</sub>O, which have well-developed (011), (0 $\bar{1}$ 1), (01 $\bar{1}$ ), and (0 $\bar{1}$  $\bar{1}$ ) faces, were grown by decreasing the temperature of a saturated aqueous solution. A single crystal of 0.30 × 0.18 × 0.18 mm<sup>3</sup> with a flat (001) surface was obtained by grinding a large single crystal into a (001) plate of ca. 0.18 mm in thickness and cutting by a razor and used for the X-ray diffraction measurements. The sample crystal on the diffractometers, an automatic four-circle diffractometer (MAC Science, MXC18HF) and a Weissenberg-type diffractometer equipped with an imaging-plate detector (MAC Science, DIP3000), was cooled in stream of cold nitrogen gas (Oxford Cryosystems, Cryostream cooler). To transform the sample into the metastable state on the diffractometers, the (001) surface was irradiated perpendicularly with a 441.6 nm line from a He–Cd laser at 110–115 K. The electric vector of the laser was set to 45° from the *a*-axis. Generation of blue color was confirmed prior to the X-ray measurements using a telescopic system of Figure 1b with crossed polarizers. The X-ray radiation used for all the measurements was graphite-monochromated MoK $\alpha$  ( $\lambda = 0.71073$  Å).

For spectroscopic measurements, *c*-cut plates of 100–200  $\mu$ m in thickness were prepared by grinding large single crystals, and surfaces of them were polished by a lapping film (Sumitomo 3M, #10000). An experimental setup for the measurements is shown in Figure 2a. The crystalline plate prepared was attached to a coldfinger, which has a light transmitting aperture of 1 mm in diameter, of a liquid nitrogen cryostat (Oxford Instruments, DN1754). To transform the sample into the metastable state, a mirror M was inserted and irradiation was done at 77 K with various wavelengths: 441.6 nm from a He–Cd laser; 457.9, 476.5, 488.0, and 514.5 nm from an Ar ion laser, and 632.8 nm from a He–Ne laser.

Polarized absorption spectra in the visible region were measured after removing the mirror M and polarizer P2. Polarizations of both the laser light and the white light were parallel to the *a*-axis.

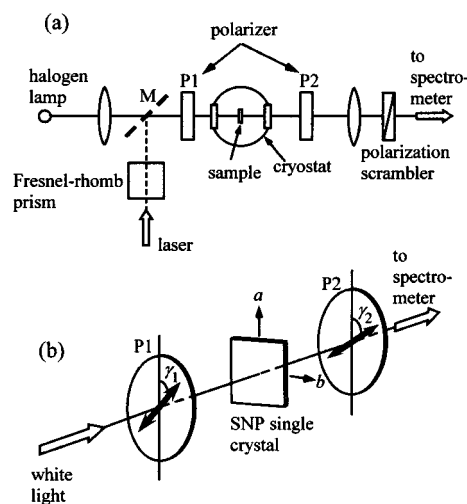


**Figure 2.** Experimental setup for spectroscopic measurements of the metastable state (a), and definitions of  $\gamma_1$  and  $\gamma_2$  (b).

For observations of the anomalous optical property illustrated in Figure 1, the optimum angle between the electric vector of laser light for excitation and the crystallographic *a*-axis,  $\chi$ , is 40–50°, which is adjusted by a Fresnel-rhomb prism and a polarizer P1. Irradiation time ranged from 30 to 120 min under laser power of 5–50 mW. Then, mirror M was removed and spectra of transmitted white light were recorded by a single polychromator of  $f = 25$  cm (Ritsu MC-25N) equipped with an ICCD detector (Princeton Instruments, ICCD-576G/1). To specify the orientation of two polarizers P1 and P2, angles  $\gamma_1$  and  $\gamma_2$  are defined as shown in Figure 2b.

## III. Results and Discussion

**A. X-ray Diffraction.** The lattice constants measured at 114 K before and after irradiation of 441.6 nm were as follows:  $a = 6.147(1)$ ,  $b = 11.847(2)$ ,  $c = 15.535(3)$  Å,  $V = 1131.3(4)$  Å<sup>3</sup> before irradiation, and  $a = 6.150(2)$ ,  $b = 11.849(3)$ ,  $c = 15.535(4)$  Å,  $V = 1132.1(5)$  Å<sup>3</sup> after irradiation. Although a slight elongation of the *a*-axis upon irradiation was observed, the change is much smaller than the elongation by ca. 0.012 Å reported by Coppens and co-workers.<sup>8</sup> This discrepancy is attributable to the difference in polarization of laser light applied for formation of the metastable state; the polarization was intermediate between the *a*- and *b*-axes in the present study, while it was parallel to the *c*-axis in ref 8. It is known that an extremely high population up to 50% of the metastable anion is obtained by the *c*-polarized light of 457.9 nm.<sup>12,13</sup> Although the population achieved by the *a*- or *b*-polarized light has not been documented clearly, it must be fairly low compared to the *c*-polarized light.

Signs of the symmetry change were searched carefully. However, any deviation from orthorhombic system in diffraction intensities, an additional reflection, or a diffuse scattering were not found. Therefore, we have concluded that the light-induced symmetry change does not occur in the short scale that can be detected by X-ray diffraction methods.

**B. Optical Properties.** Electronic absorption spectra are shown in Figure 3. Upon irradiation, a new broad band characteristic to the metastable state appears at 660 nm. Intensity of the band in the 457.9 nm excitation is much stronger compared to the 488 nm excitation, which reflects the high population of the metastable anion. It should be noted that there are no anomalies in the absorption spectra around the excitation wavelengths, 488 and 457.9 nm.

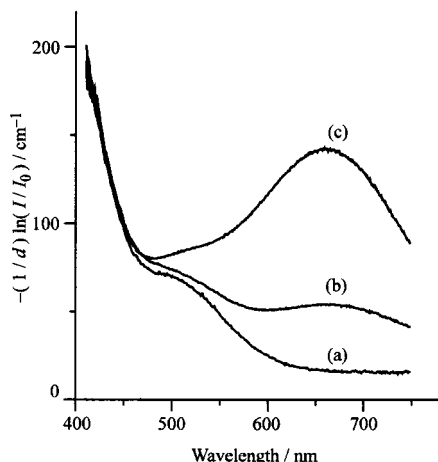


**Figure 3.** Absorption spectra of the ground state (a); and the metastable state produced by 488 nm irradiation (b), and 457.9 nm irradiation (c). The temperature of the sample was 77 K. The electric vectors of both the lasers applied to produce the metastable state and the white light source for the spectroscopic measurements are parallel to the  $a$ -axis. The symbol  $d$  in the label of the vertical axis denotes thickness of the sample.

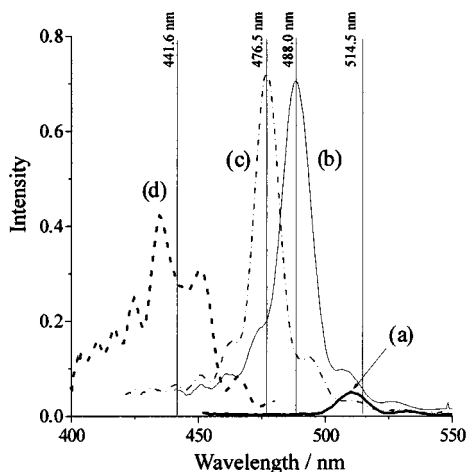


**Figure 4.** Band-pass filter characteristics of a  $c$ -cut SNP crystal in the metastable state placed between crossed polarizers. The crystal was 142  $\mu\text{m}$  in thickness and was irradiated with 514.5 nm (a), 488.0 nm (b), 476.5 nm (c), and 441.6 nm (d) laser lines. The vertical axis is the fraction of intensity of light that is transmitted through crossed polarizers, i.e.,  $I_{\text{cross}}/(I_{\text{parallel}} + I_{\text{cross}})$ . Wavelengths of the laser lines are shown by vertical lines. The irradiation and spectroscopic measurements were carried out at 77 K.

Spectra of the transmitted light through the SNP crystal sandwiched between crossed polarizers ( $\gamma_1 = 0^\circ$ ,  $\gamma_2 = 90^\circ$ ) after irradiations with 514.5, 488.0, 476.5, and 441.6 nm lines of  $\chi = 45^\circ$  are shown in Figure 4. The same sample of 142  $\mu\text{m}$  thick was used in these spectra. The spectra a, b, and c are quasi-monochromatic with half-widths of 20–30 nm, and the spectrum d is of multiple peaks. Spectral shape depends on not only the laser wavelength but also on the sample thickness. Experiments on the thickness dependency of the spectra, however, were not successful because of the difficulty in preparing thin plates of desired thickness. A remarkable point is that the peak wavelength  $\lambda_0$  coincides with the wavelength of the applied laser ( $\lambda_L$ ) within an error of 1 nm in the spectra on irradiations with 488 (b) and 476.5 nm (c), while  $\lambda_0$  and  $\lambda_L$  differ by about 10 nm in our previous study.<sup>10</sup> The discrepancy between the present and the previous experiments may be attributable to the effect of the white light sources for the measurements of the spectra. The white light gradually affects the population of the metastable

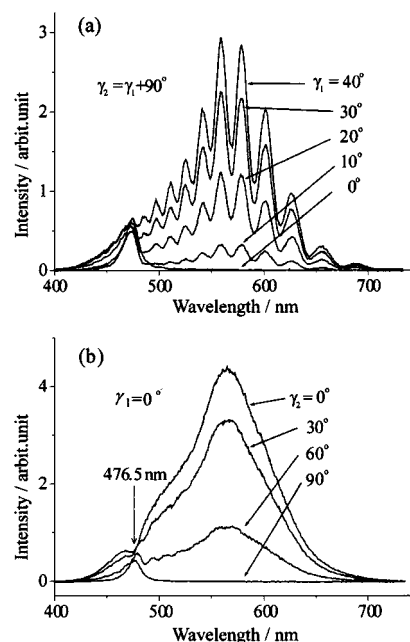


**Figure 5.** Spectra of transmitted white light in various angles of  $\gamma_1$  and  $\gamma_2$ , which are defined in Figure 2. The metastable state was produced by 476.5 nm irradiation. The polarizers are crossed in (a), and  $\gamma_1$  is fixed to  $0^\circ$  in (b). The irradiation and spectroscopic measurements were carried out at 77 K.

anion. In the experiments in ref 10, only a single channel spectrometer and optics of low throughput were available and, therefore, relatively high power of the white light and long measuring time was required to obtain one spectrum covering the visible region. In the present experiment, on the other hand, the power of white light and a measuring time were reduced significantly, since a highly efficient spectrometer was available. Thus, the present results show that the band center  $\lambda_0$  is precisely equal to the wavelength of laser light applied for the metastable state formation, i.e.,

$$\lambda_0 = \lambda_L \quad (3.1)$$

when disturbance by the white light is not significant. On the basis of the accidental isotropy in optically active crystals,  $\lambda_0$  is the wavelength in which refractive indices for the  $a$  and  $b$  axes,  $n_a$  and  $n_b$ , coincide with each other. Although it is not unusual that the refractive indices change with  $\lambda_L$ , since the population of the metastable anion depends on  $\lambda_L$ , the equality eq 3.1 is puzzling.

The absence of the symmetry change shown by the X-ray diffraction and the equality between  $\lambda_0$  and  $\lambda_L$  suggest that the accidental isotropy model should be discarded. To our knowledge, the phenomenon shown in Figure 4, especially the equality between  $\lambda_0$  and  $\lambda_L$ , which is paraphrased as “wavelength of a laser is printed or memorized in a crystal”, is not known so far. To investigate this interesting phenomenon, which is referred to as “wavelength printing effect” hereafter, the polarization of the transmitted white light was examined by the setup shown in Figure 2 with various orientations of P1 and P2. Spectra of the transmitted light under crossed polarizers at various angles of  $\gamma_1$  are shown in Figure 5a. The sample is a  $c$ -cut crystal of 200  $\mu\text{m}$  in thickness after irradiation with 476.5 nm line from an Ar ion laser with a polarization  $\chi = 45^\circ$ . In wavelength regions  $\lambda < 420$  nm and  $\lambda > 520$  nm, intensity changes with  $\gamma_1$  like ordinary birefringent crystals and the extinction occurs when P1 and P2 are directed to the crystallographic  $a$  and  $b$  axes ( $\gamma_1$

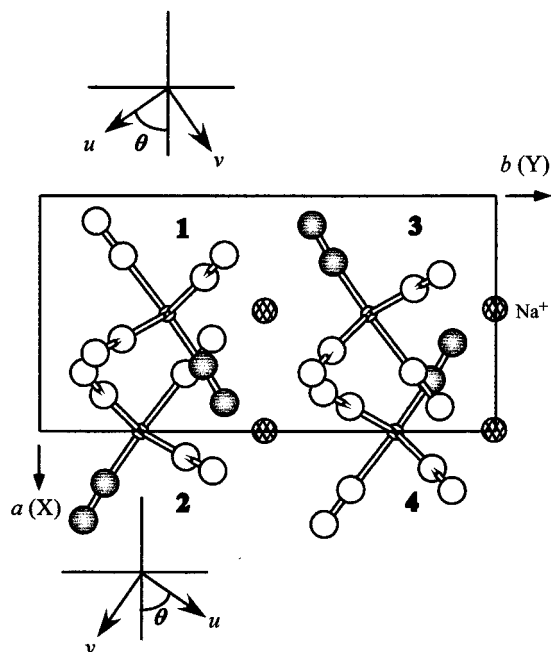


**Figure 6.** Arrangement of  $[\text{Fe}(\text{CN})_5\text{NO}]\cdot\text{H}_2\text{O}$  anions in the crystal. Four anions are contained in a unit cell of  $Pnm$  space group. Molecular coordinates  $u$  and  $v$  are perpendicular and parallel to the Fe–N–O axis, respectively.

$= 0^\circ$ ,  $\gamma_2 = 90^\circ$ ). In the anomalous region,  $420 \text{ nm} < \lambda < 520 \text{ nm}$ , however, there is no extinction direction for the crossed-polarizers. Spectra of the transmitted light at various angles of  $\gamma_2$  and fixed  $\gamma_1 (= 0^\circ)$  are shown in Figure 5b. This figure shows that the transmitted light of the anomalous region is not linearly polarized but elliptically polarized, because it does not become extinct at any angles of  $\gamma_2$ . The ratio of intensities at  $\gamma_2 = 0^\circ$  and  $\gamma_2 = 90^\circ$  in the anomalous region varies depending on the sample thickness and the wavelength of the laser.

The features of the anomalous region cannot be explained based on the optical properties of homogeneous crystals, and a spatially heterogeneous structure should be considered. The polarization of the incident laser may vary along the propagation direction due to the retardation of the optically anisotropic crystal, and population of the metastable anion may depend on the polarization of the laser. Since polarizabilities of the metastable state and ground state anions are different from each other, it is a plausible assumption that the spatially heterogeneous refractive indices might be generated. In the following section, a mechanism of the wavelength printing effect comprised of photorefractive formation of a spatially modulated refractive indices is proposed.

### C. Mechanism of the Wavelength Printing Effect. 1.

*Orientation Modulation of Principal Axes of Refraction Owing to the Population of the Metastable State.* The crystal structure of SNP projected on the (001) plane is shown in Figure 6. Cartesian coordinates ( $X$ ,  $Y$ ,  $Z$ ) are chosen parallel to the crystallographic  $a$ ,  $b$ , and  $c$  axes. The  $C_4$  axis of the  $[\text{Fe}(\text{CN})_5\text{NO}]^{2-}$  anion having approximate  $C_{4v}$  symmetry is perpendicular to the  $c$ -axis. As discussed by Guida et al.,<sup>16</sup> the highest population of the metastable anion upon irradiation with  $c$ -polarized light suggests that an electronic excitation by the light polarized perpendicularly to the  $C_4$  axis is considered to be the main pathway to the metastable anion. We define the molecular coordinates  $u$  and  $v$  that are perpendicular and parallel to the  $C_4$  axis, respectively (see Figure 6). Because pairs of anions, **1** and **3**, and **2** and **4**, which are related by inversion centers, are equivalent concerning the following discussion on

the excitation rate by the polarized light, only two anions at sites **1** and **2** are taken into consideration explicitly. The anions at sites **1** and **2** are related to each other by a glide plane perpendicular to the  $b$  axis. The angle made by  $u$  and  $X$  is about  $53^\circ$  and is denoted by  $\theta$ . To simplify the analysis, we ignore  $\text{MS}_2$ , since we have shown that  $\text{MS}_2$  is not essential for the wavelength printing effect.<sup>17</sup>

Our model, which describes how the wavelength printing effect occurs, includes following two parts: (1) a population difference of the metastable anion between sites **1** and **2** is generated and the difference varies periodically in the SNP crystal; (2) the modulated population difference causes a modulation of the orientation of the principal axes of refraction and makes the SNP crystal in the metastable state something similar to a pile of identical retardation plates of birefringent material in the Sölc filter. Such a pile of retardation plates, in which the principal axes of refraction are rotated by a small angle in both senses alternatively, placed between two polarizers acts as a band path filter.<sup>14,15</sup>

To investigate the population difference mentioned above, we express the electric field of laser light traveling along the  $c$ -axis by

$$\begin{aligned} E_X &= A_X \exp(-i\omega t) \\ E_Y &= A_Y \exp(-i\omega t) \end{aligned} \quad (3.2)$$

where  $A_X$  and  $A_Y$  are complex amplitudes and  $\omega$  is angular frequency of light. The complex amplitudes  $A_X$  and  $A_Y$  are functions of  $z$ . Time-averaged energy fluxes of  $u$  and  $v$  components of the electric field exerted on the anions are proportional to the following quantities:

$$\begin{aligned} J_{1u} &= |A_X|^2 \cos^2 \theta + |A_Y|^2 \sin^2 \theta - \\ &\quad (A_X A_Y^* + A_Y A_X^*) \cos \theta \sin \theta \\ J_{1v} &= |A_X|^2 \sin^2 \theta + |A_Y|^2 \cos^2 \theta + \\ &\quad (A_X A_Y^* + A_Y A_X^*) \cos \theta \sin \theta \end{aligned} \quad (3.3)$$

for the anion at site **1**, and

$$\begin{aligned} J_{2u} &= |A_X|^2 \cos^2 \theta + |A_Y|^2 \sin^2 \theta + \\ &\quad (A_X A_Y^* + A_Y A_X^*) \cos \theta \sin \theta \\ J_{2v} &= |A_X|^2 \sin^2 \theta + |A_Y|^2 \cos^2 \theta - \\ &\quad (A_X A_Y^* + A_Y A_X^*) \cos \theta \sin \theta \end{aligned} \quad (3.4)$$

for the anion at site **2**. Light-induced conversion between GS and  $\text{MS}_1$  is caused by the action of the energy flux given above and the population of  $\text{MS}_1$  changes with time. Kinetic equations for the fractional populations of  $\text{MS}_1$  at site **1** and site **2**, which are denoted by  $p_1$  and  $p_2$ , respectively, under the irradiation are expressed by

$$\begin{aligned} \frac{dp_1}{d\tau} &= \{k_{u+}(1-p_1) - k_{u-p_1}\}J_{1u} + \\ &\quad \{k_{v+}(1-p_1) - k_{v-p_1}\}J_{1v} \\ \frac{dp_2}{d\tau} &= \{k_{u+}(1-p_2) - k_{u-p_2}\}J_{2u} + \\ &\quad \{k_{v+}(1-p_2) - k_{v-p_2}\}J_{2v} \end{aligned} \quad (3.5)$$

where  $\tau$  denotes the irradiation time of the laser. Kinetic



constants  $k_{u+}$  and  $k_{v+}$  are transition rates from GS to MS<sub>1</sub> through absorption of the  $u$  and  $v$  polarized components of light, whereas  $k_{u-}$  and  $k_{v-}$  stand for the rates from MS<sub>1</sub> to GS.

To discuss the effects of the population of the metastable anion on the optical property of the SNP crystal in its metastable state, we express the polarizability tensor of the anion by

$$\alpha = \begin{pmatrix} (1-p)\alpha_{\text{GS}}^u + p\alpha_{\text{MS}}^u & 0 \\ 0 & (1-p)\alpha_{\text{GS}}^v + p\alpha_{\text{MS}}^v \end{pmatrix}_{(uv)} \quad (3.6)$$

The subscript  $(uv)$  in the right-hand side indicates the basis coordinate of the matrix. Off-diagonal elements are zero since the  $C_{4v}$  symmetry is retained in MS<sub>1</sub>.<sup>8</sup> The dielectric tensor for the optical region is given by

$$\epsilon = \epsilon_0 \mathbf{I} + \mathbf{P}/\mathbf{E} = \epsilon_0 \mathbf{I} + (N/2)(\alpha_1 + \alpha_2 + 4\alpha_{\text{Na}^+} + 4\alpha_{\text{H}_2\text{O}}) \quad (3.7)$$

in which  $\alpha_1$  and  $\alpha_2$  are the polarizability tensors of [Fe(CN)<sub>5</sub>-NO]<sup>2-</sup> anions at sites **1** and **2**;  $\alpha_{\text{Na}^+}$  and  $\alpha_{\text{H}_2\text{O}}$  are the polarizability tensors of Na<sup>+</sup> and H<sub>2</sub>O, respectively;  $N$  is the number of formula units in a unit volume;  $\epsilon_0$  is the dielectric constant of vacuum; and  $\mathbf{I}$  is a unit tensor. In this expression, the local field correction is ignored, because it must not be essential in the present problem. Performing appropriate transformation of eq 3.6 to the Cartesian coordinate for the site **1** and site **2** anions, eq 3.7 on the basis of the Cartesian coordinate becomes

$$\epsilon = \begin{pmatrix} \epsilon_X & \epsilon_{XY} \\ \epsilon_{XY} & \epsilon_Y \end{pmatrix}_{(XY)} \quad (3.8)$$

where

$$\begin{aligned} \epsilon_X &= \epsilon_0 + \epsilon' + (N/2)\{((2-p_1-p_2)\alpha_{\text{GS}}^u + (p_1+p_2)\alpha_{\text{MS}}^u)\cos^2\theta + ((2-p_1-p_2)\alpha_{\text{GS}}^v + (p_1+p_2)\alpha_{\text{MS}}^v)\sin^2\theta\} \\ \epsilon_Y &= \epsilon_0 + \epsilon' + (N/2)\{((2-p_1-p_2)\alpha_{\text{GS}}^u + (p_1+p_2)\alpha_{\text{MS}}^u)\sin^2\theta + ((2-p_1-p_2)\alpha_{\text{GS}}^v + (p_1+p_2)\alpha_{\text{MS}}^v)\cos^2\theta\} \\ \epsilon_{XY} &= (p_1-p_2)(\alpha_{\text{GS}}^u - \alpha_{\text{GS}}^v - \alpha_{\text{MS}}^u + \alpha_{\text{MS}}^v)\cos\theta\sin\theta \quad (3.9) \end{aligned}$$

The symbol  $\epsilon' \equiv (N/2)(4\alpha_{\text{Na}^+} + 4\alpha_{\text{H}_2\text{O}})$  is introduced assuming isotropic polarizabilities of Na<sup>+</sup> and H<sub>2</sub>O.

Populations,  $p_1$  and  $p_2$ , of the metastable anion depend on the energy flux of laser light as eq 3.5. At the same time, propagation of the laser light is controlled by the dielectric tensor eqs 3.8 and 3.9, which depend on  $p_1$  and  $p_2$ . Before considering such a complicated problem, it may be valuable to have insight into the wavelength printing effect to discuss a simpler situation in which propagation of laser light is not affected by the population of the metastable anion and the populations  $p_1$  and  $p_2$  are proportional to  $J_{1u}$  and  $J_{2u}$ , respectively. The latter approximation corresponds to the case in which the populations of the metastable state anion are much less than the saturation level and are approximated by

$$\begin{aligned} p_1 &\cong k_{u+}J_{1u}\Delta\tau \\ p_2 &\cong k_{u+}J_{2u}\Delta\tau \quad (3.10) \end{aligned}$$

In such a case,  $A_X$  and  $A_Y$  in eq 3.2 can be written as

$$\begin{aligned} A_X &= A_0 \exp(2\pi i n_a z / \lambda_L) \\ A_Y &= A_0 \exp(2\pi i n_b z / \lambda_L) \quad (3.11) \end{aligned}$$

where  $A_0$  is a real constant,  $n_a$  and  $n_b$  are refractive indices, and  $\lambda_L$  is the wavelength of laser light in a vacuum. This expression corresponds to the linearly polarized light with the electric vector directed to 45° from the  $a$ -axis at the front surface of the sample ( $z = 0$ ). Energy fluxes, eqs 3.3 and 3.4 in this case, are reduced to

$$\begin{aligned} J_{1u} &= A_0^2(1 - 2\cos\theta\sin\theta\cos\phi) \\ J_{2u} &= A_0^2(1 + 2\cos\theta\sin\theta\cos\phi) \quad (3.12) \end{aligned}$$

where  $\phi$  represents the phase difference  $2\pi(n_a - n_b)z/\lambda_L$ . From eqs 3.10 and 3.12,  $p_1 + p_2 = 2(k_{u+}\Delta\tau)A_0^2$  is independent of  $z$ , but  $p_1 - p_2 = -4(k_{u+}\Delta\tau)A_0^2\cos\theta\sin\theta\cos\phi$  depends on  $z$  through the phase difference  $\phi$ . Therefore,  $\epsilon_X$  and  $\epsilon_Y$  are independent of  $z$ , whereas  $\epsilon_{XY}$  depends on  $z$  as

$$\begin{aligned} \epsilon_{XY} &= -4(k_{u+}\Delta\tau)A_0^2(\alpha_{\text{GS}}^u - \alpha_{\text{GS}}^v - \alpha_{\text{MS}}^u + \\ &\alpha_{\text{MS}}^v)\cos^2\theta\sin^2\theta\cos(2\pi(n_a - n_b)z/\lambda_L) \quad (3.13) \end{aligned}$$

The nonzero value of  $\epsilon_{XY}$  causes a small rotation of the principal axes by

$$\Delta \equiv \tan^{-1}(\epsilon_{XY}/|\epsilon_X - \epsilon_Y|) \quad (3.14)$$

in both sense depending on the sign of  $\cos(2\pi(n_a - n_b)z/\lambda_L)$ .

This situation closely resembles the Sölc filter, which was first developed by Sölc and investigated by Evans theoretically.<sup>14,15</sup> The Sölc filter is a pile of identical retardation plates of birefringent material placed between crossed polarizers. The principal axes of the  $j$ th plate should be rotated alternatively to the transmitting direction of the first polarizer by small angles  $\delta_j = (-1)^j|\delta|$ . Evans has shown that wavelength of the principal transmission band is given by

$$\lambda_0 = 2d\Delta n \quad (3.15)$$

where  $d$  is a thickness of a single retardation plate and  $\Delta n$  is the difference of refractive indices of the retardation plate. Since the modulation period of the Sölc filter  $2d$  corresponds to  $\lambda_L/(n_a - n_b)$  (see eq 3.13) in the present material and  $\Delta n = n_a - n_b$ , eq 3.15 indicates that wavelength transmitted by the system shown in Figure 1 equals the wavelength of laser light applied to produce the metastable state, i.e.  $\lambda_0 = \lambda_L$ . This equality is considered to correspond to the observed equality eq 3.1.

**2. Photostationary State.** Although the analysis in the previous section must have shown the essential point of the wavelength printing effect, it is not enough to be applied to the photostationary state in which experimental observations were performed. The conditions of the photostationary state,  $dp_1/d\tau = 0$  and  $dp_2/d\tau = 0$ , are expressed by

$$\begin{aligned} p_1 &= \frac{k_{u+}J_{1u} + k_{v+}J_{1v}}{(k_{u+} + k_{u-})J_{1u} + (k_{v+} + k_{v-})J_{1v}} \\ p_2 &= \frac{k_{u+}J_{2u} + k_{v+}J_{2v}}{(k_{u+} + k_{u-})J_{2u} + (k_{v+} + k_{v-})J_{2v}} \quad (3.16) \end{aligned}$$

If  $k_{v+}$  and  $k_{v-}$  were zero or  $k_{u+}$  and  $k_{u-}$  were zero,  $p_1$  and  $p_2$

should be independent of  $z$  and, therefore, the modulation of  $\epsilon_{XY}$  should not occur in the photostationary state. A more serious problem is that eq 3.11 cannot be used for evaluation of  $J_{1u}$  etc., because refractive indices change in time and space with  $p_1$  and  $p_2$  under irradiation. Therefore, we investigated effects of continued irradiation by a numerical method. The calculation procedure is as follows. Putting zeros in  $p_1$  and  $p_2$  of eqs 3.8 and 3.9 for all  $z$ ,  $z$ -dependent complex amplitudes  $A_X$  and  $A_Y$  are calculated for  $z = j\Delta z$ ,  $j = 1, 2, 3, \dots$  using Berreman's  $4 \times 4$  matrix method.<sup>18</sup> Population of the metastable anion  $p_1$  and  $p_2$  as functions of  $z$  are calculated assuming that energy flux does not change for a short interval of time  $\Delta\tau$  using eqs 3.3, 3.4 and

$$\Delta p_i = [\{k_{u+}(1 - p_i) - k_{u-}p_i\}J_{iu} + \{k_{v+}(1 - p_i) - k_{v-}p_i\}J_{iv}]\Delta\tau \quad (3.17)$$

where  $i = 1, 2$ . The dielectric tensor eq 3.9 is renewed based on the calculated  $p_i$ , thus the first  $\tau$ -step is finished. The second  $\tau$ -step begins with the calculation of  $A_X$  and  $A_Y$  based on the renewed dielectric tensor for the next time interval. These steps are followed successively until the electric field and the population become stationary. Berreman's  $4 \times 4$  matrix method is a technique to solve numerically Maxwell's equation for the electromagnetic wave. The  $z$ -dependent complex amplitudes  $A_X$  and  $A_Y$  in eq 3.2 can be calculated for an anisotropic medium having a  $z$ -dependent dielectric tensor. The value of  $\Delta z$  in the  $4 \times 4$  calculation was set to  $0.005 \times \lambda_L$ . The parameter  $(|A_X|^2 + |A_Y|^2)k_{u+}\Delta\tau$ , which appears in the combined equation of eqs 3.3, 3.4, and 3.17 and is independent of both  $z$  and  $\tau$ , was set to 0.05 tentatively. The value of  $\epsilon'$  in eq 3.9 was estimated to  $0.16 \epsilon_0$  from molar polarizability data of  $\text{Na}^+$ ,  $0.29 \times 10^{-24} \text{ cm}^3 \times (4\pi\epsilon_0)$ ,<sup>19</sup> and of  $\text{H}_2\text{O}$ ,  $1.47 \times 10^{-24} \text{ cm}^3 \times (4\pi\epsilon_0)$ , which is derived from the refractive index of water. Parameters connected to the polarizabilities of the ground-state anion  $(N/2\epsilon_0)\alpha_{\text{GS}}^u$  and  $(N/2\epsilon_0)\alpha_{\text{GS}}^v$  were estimated to 0.53 and 0.84, respectively, based on the reported refractive indices,  $n_a = 1.6150$  and  $n_b = 1.5619$ .<sup>20</sup> Polarizability parameters  $(N/2\epsilon_0)\alpha_{\text{MS}}^u = 0.53$  and  $(N/2\epsilon_0)\alpha_{\text{MS}}^v = 0.95$ , and those of relative kinetic parameters  $k_{u-}/k_{u+} = 8.0$ ,  $k_{v+}/k_{u+} = 0$ , and  $k_{v-}/k_{u+} = 4.0$  were evaluated arbitrarily, since no experimental data are available. Therefore, discussion based on the present calculation is limited to the qualitative area. The procedure above is a simulation of approaching the photostationary state under continued irradiation with laser light of wavelength  $\lambda_L$ . Therefore, we put  $A_X/A_Y = 1$  at the front surface of the sample ( $z = 0$ ). This procedure will be referred to as "populating stage" hereafter.

Intensities of  $I_X$ ,  $I_Y$ , and  $p_1$  as functions of  $z$  after the populating stage of increasing  $\tau$ -steps are shown in Figure 7, where  $I_X$  and  $I_Y$  mean intensities of  $X$  and  $Y$  components. The population at site 2,  $p_2$ , is not shown, because it is almost same as  $p_1$  except it is the opposite phase. The populating stage of one  $\tau$ -step corresponds to the simplified scheme using eqs 3.10 and 3.11, which leads to a sinusoidal population wave for  $p_1$  with a period of  $\lambda_L/|n_a - n_b| \equiv \lambda_p$  (Figure 7a). As the  $\tau$ -step increases,  $I_X/I_Y$  deviates from 1. This is due to the property similar to the optical rotatory power revealed by the modulated orientation of the optical indicatrix, which causes an irregular change of the population wave  $p_1$  (Figure 7b and c). On further  $\tau$ -steps, however, the relation of  $I_X/I_Y \approx 1$  recovers and  $p_1$  comes to have a regular waveform again (Figure 7d). This state is considered to be the photostationary state reached under the continued irradiation, since additional  $\tau$ -steps do not cause

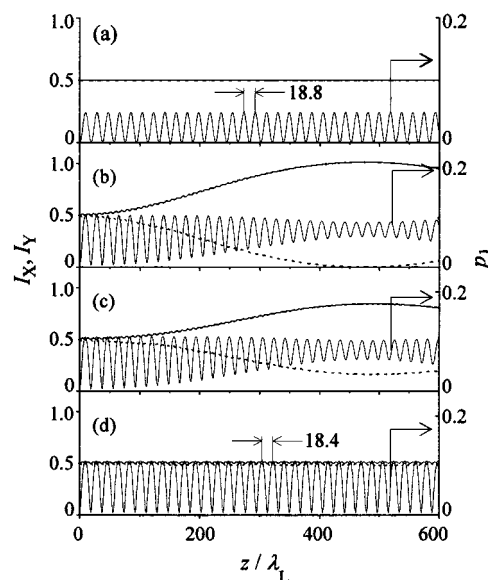


**Figure 7.** Spatial changes of  $I_X$  (dotted lines),  $I_Y$  (solid lines), and  $p_1$  at populating stage. Parameters used are as follows:  $(N/2\epsilon_0)\alpha_{\text{GS}}^u = 0.53$ ,  $(N/2\epsilon_0)\alpha_{\text{GS}}^v = 0.84$ ,  $(N/2\epsilon_0)\alpha_{\text{MS}}^u = 0.53$ ,  $(N/2\epsilon_0)\alpha_{\text{MS}}^v = 0.95$ ,  $k_{u-}/k_{u+} = 8.0$ ,  $k_{v+}/k_{u+} = 0$ , and  $k_{v-}/k_{u+} = 4.0$ . Number of  $\tau$ -steps are 1 (a), 5 (b), 10 (c), and 100 (d). The wave of  $p_1$  has a period of  $18.8 \lambda_L$  in (a) and  $18.4 \lambda_L$  in (d).

significant changes. The decrease of  $\lambda_p$  from  $18.8 \lambda_L$  in Figure 7a to  $18.4 \lambda_L$  in Figure 7d is due to the assumed relation of  $\alpha_{\text{MS}}^v > \alpha_{\text{GS}}^v$ , which increases  $|n_a - n_b|$  as the metastable anion populates.

To simulate experiments of the wavelength printing effect in which incident white light is  $a$ -polarized, a condition of  $A_Y = 0$  at  $z = 0$  is applied and the parameter  $(|A_X|^2 + |A_Y|^2)k_{u+}\Delta\tau$  is set to zero to inhibit further changes. In the photostationary state Figure 7d, the rotation angle of the principal axes of refraction,  $\Delta$  in eq 3.14, varies with  $z$  as shown in Figure 8a. The  $\Delta$ -wave has a period of  $\lambda_p$  and an amplitude of  $0.034$  ( $1.9^\circ$ ). Polarization changes of the incident  $a$ -polarized light are shown in Figure 8b for the wavelengths  $\lambda = 0.8 \lambda_L$ ,  $0.95 \lambda_L$ , and  $\lambda_L$ . The polarization state changes with  $z$ , and the most significant change takes place for the light of  $\lambda = \lambda_L$ . This point is shown clearly in Figure 8c, in which intensities of  $b$ -polarized components  $I_Y$  at  $z = 100 \lambda_L$ (A),  $283 \lambda_L$ (B), and  $450 \lambda_L$ (C) are plotted as functions of  $\lambda$ . Symbols A, B, and C correspond to positions A, B, and C in Figure 8b. The value of  $z$  at B,  $283 \lambda_L$ , is the optimum thickness of a sample for the band-pass characteristic shown in the experiment of Figure 1. A peak position of the  $I_Y$  curve in Figure 8b, which is denoted by  $z_{\text{max}}$ , depends on the amplitude of the  $\Delta$ -wave. In the Sölc filter, an optimum condition for the number of retardation plates  $n$  and rotation angle of the plate  $|\delta|$  is given by  $n = (\pi/4)(1/|\delta|)$ .<sup>15</sup> Because twice the thickness of the retardation plate in the Sölc filter should be related to  $\lambda_p$  in the present calculation, an expected value of  $z_{\text{max}}$  is  $\lambda_p \times (\pi/8)(1/|\delta|) = 212 \lambda_L$ , in which  $|\delta|$  is regarded as the amplitude of the  $\Delta$ -wave,  $0.034$ . The difference between  $283 \lambda_L$  and  $212 \lambda_L$  is attributable to the difference in the forms of the  $\Delta$ -wave, namely the rectangular wave in the Sölc filter instead of Figure 8a. Apart from the difference above, the analogy with the Sölc filter suggests that the  $z_{\text{max}}$  varies inversely as the amplitude of the  $\Delta$ -wave.

In the viewpoint of the present calculations, the observed band-pass characteristics revealed by the metastable state of SNP shown Figure 4 can be interpreted as follows. The spectra at  $488.0$  and  $476.5$  nm irradiation (Figure 4b and c) are close to

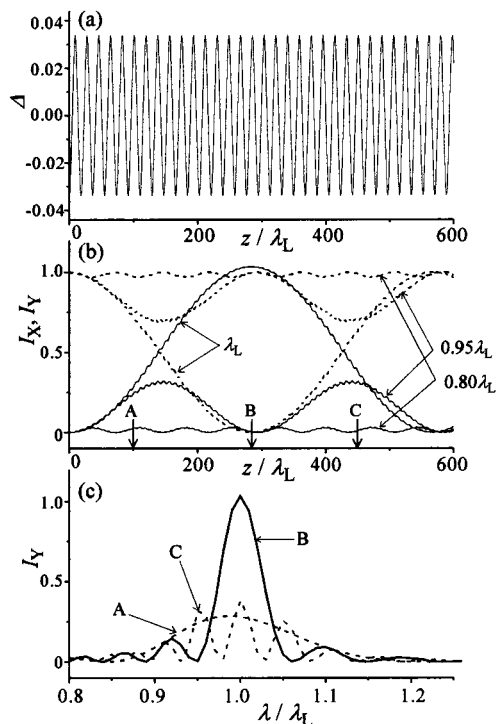


**Figure 8.** Optical properties of the state Figure 7d. Spatial change of the rotation angle of the principal axes of refraction,  $\Delta$  (a); spatial changes of  $I_x$  (dotted lines) and  $I_y$  (solid lines) for  $a$ -polarized incident light with wavelengths  $\lambda = 0.8 \lambda_L$ ,  $0.95 \lambda_L$ , and  $\lambda_L$  (b); spectra of  $b$ -polarized component ( $I_y$ ) at  $z = 100 \lambda_L$  (A),  $283 \lambda_L$  (B), and  $450 \lambda_L$  (C) (c).

the optimum case B in Figure 8. Population of the metastable anion and an amplitude of the  $\Delta$ -wave at 514.5 nm irradiation is much less than those at 488.0 and 476.5 nm irradiations. Therefore, the  $z_{\max}$  value is much larger for 514.5 nm than for 488.0 and 476.5 nm irradiations, which gives rise to a spectrum similar to A in Figure 8c at the same thickness of the sample. On the contrary, higher population under the 441.6 nm light brings about a spectrum with multiple peaks similar to C in Figure 8c.

#### IV. Conclusion

A new phenomenon revealed by the metastable state of the SNP crystal, the wavelength printing effect, is explained by assuming that an orientation modulation of the principal axes of refraction is formed in the metastable state. Numerical calculations based on Maxwell's equation and kinetic equations for the interconversion of the ground and metastable states have shown that the modulation exists even in the photostationary state.

#### References and Notes

- (1) Hauser, U.; Oestreich, V.; Rohrweck, H. D. *Z. Phys. A* **1977**, *280*, 17.
- (2) Guida, J. A.; Piro, O. E.; Aymonino, P. J. *Inorg. Chem.* **1995**, *34*, 4113.
- (3) Morioka, Y.; Ishikawa, A.; Tomizawa, H.; Miki, E. *J. Chem. Soc., Dalton Trans.* **2000**, 781.
- (4) Krasser, W.; Woike, Th.; Haussühl, S.; Kuhl, J.; Breitschwerdt, A. *J. Raman Spectrosc.* **1986**, *17*, 83.
- (5) Morioka, Y.; Hamaguchi, H. *J. Phys. Chem. Solids* **1992**, *53*, 967.
- (6) Morioka, Y.; Takeda, S.; Tomizawa, H.; Miki, E. *Chem. Phys. Lett.* **1998**, *292*, 625.
- (7) Zöllner, H.; Krasser, W.; Woike, Th.; Haussühl, S. *Chem. Phys. Lett.* **1989**, *161*, 497.
- (8) Carducci, M. D.; Pressprich, M. R.; Coppens, P. *J. Am. Chem. Soc.* **1997**, *119*, 2669.
- (9) Delly, B.; Schefer, J.; Woike, Th. *J. Chem. Phys.* **1997**, *107*, 10067.
- (10) Morioka, Y. *Solid State Commun.* **1992**, *82*, 505.
- (11) Hobden, M. V. *Acta Crystallogr. A* **1968**, *24*, 676.
- (12) Hauser, U.; Oestreich, V.; Rohrweck, H. D. *Z. Phys. A* **1978**, *284*, 9.
- (13) Woike, Th.; Krasser, W.; Zöllner, H.; Kirchner, W.; Haussühl, S. *Z. Phys. D* **1993**, *25*, 351.
- (14) Sölc, I. *Czechoslov. Cosopis pro Fysiku* **1953**, *3*, 366. Sölc, I. *Czechoslov. Cosopis pro Fysiku* **1954**, *4*, 607. Sölc, I. *Czechoslov. Cosopis pro Fysiku* **1955**, *5*, 114.
- (15) Evans, J. W. *J. Opt. Soc. Am.* **1958**, *48*, 142.
- (16) Guida, J. A.; Piro, O. E.; Aymonino, P. J. *Solid State Commun.* **1986**, *57*, 175.
- (17) Morioka, Y. *Spectrochim. Acta* **1994**, *50A*, 1499.
- (18) Berreman, D. W. *J. Opt. Soc. Am.* **1972**, *62*, 502.
- (19) Jaswal, S. S.; Sharma, T. P. *J. Phys. Chem. Solids* **1973**, *34*, 509.
- (20) Woike, Th.; Haussühl, S.; Sugg, B.; Rupp, R. A.; Beckers, J.; Imlau, M.; Schieder, R. *Appl. Phys. B* **1996**, *63*, 243.